Chemically Decoupled Nuclei in Five Lenticular Galaxies from SAURON Data

O. K. Sil'chenko[*]

Sternberg Astronomical Institute, Universitetskiĭ pr. 13, Moscow, 119992 Russia

Received October 12, 2004

Abstract—We analyze data from the SAURON integral-field spectrograph of the William Herschel 4-m telescope for five lenticular galaxies in which we previously found chemically decoupled nuclei from observations with the Multipupil Fiber Spectrograph of the 6-m Special Astrophysical Observatory telescope. In a larger field of view, we confirmed the presence of peaks of the equivalent width of the Mg Ib $\lambda5175$ absorption line in the nuclei of all five galaxies. However, the structure of the chemically decoupled regions turned out to be highly varied even in such a small sample: from compact unresolved knots to disks with an extent of several hundred parsecs and, in one case, a triaxial compact minibar-type structure. We confirmed the presence of an inner gaseous polar ring in NGC 7280 and found it in NGC 7332. In their outer parts, the planes of these polar rings are warped toward the plane of stellar rotation in such a way that the gas counterrotates with respect to the stars. This behavior of the gas in a triaxial potential was predicted by several theoretical models. © *2005 Pleiades Publishing, Inc.*

Key words: *galaxies, groups and clusters of galaxies, galactic nuclei, galaxy structure, galaxy evolution.*

INTRODUCTION

In 1992, we published a paper (Sil'chenko *et al.* 1992) in which we reported the discovery of chemically decoupled nuclei in several disk galaxies of early types, from S0 to Sb. This discovery was the result of the very first (test) observations with the MPFS (Multipupil Fiber Spectrograph) integral-field spectrograph designed for the 6-m Special Astrophysical Observatory (SAO) telescope. MPFS was among the first integral-field instruments in the world. Spectrographs of this type implied a transition to qualitatively new spectroscopic studies of galaxies, since they allowed one to take spectra from each point of an object's extended region during a single exposure and over a wide wavelength range and, thus, to effectively compare the spectral characteristics at different locations of the region under study. The first version of MPFS (Afanasiev *et al.* 1990) was put into operation in 1989 and worked until 1993. Its optics was not too transparent, and its detector, the Kvant panoramic photon counter, was not too efficient for high-surface-brightness galaxies. Therefore, our results published in 1992 were not two-dimensional maps, but azimuthally averaged radial profiles of the equivalent widths of strong absorption lines in the integrated spectra of galaxies, Mg Ib $\lambda5175$

and Fe I+Ca I $\lambda5270$. However, since we had two-dimensional rather than one-dimensional (long-slit) spectroscopic data from the outset, we were able to maintain an approximately constant signal-to-noise ratio along the radius up to an angular distance of $5''-6''$ from the center and, thus, to estimate the spectral characteristics of the stellar nuclei of galaxies and nearby regions of their bulges by adding the spectra in rings. In 1989–1990, we observed 12 bright galaxies with morphological types from E to Sb and found chemically decoupled nuclei in seven of them: the equivalent width of the Mg Ib absorption line in the nucleus was more than 1 Å larger than its equivalent width in the nearest regions of the bulge; at the then existing accuracy of the azimuthally averaged equivalent widths, 0.3 Å, this was a significant effect. At that time, we tentatively interpreted this effect as evidence of an enhanced metallicity in the compact (unresolved) stellar nuclei of galaxies. Basically, the metallicity gradients along the radius of spheroidal stellar systems, which the elliptical galaxies and the bulges of disk galaxies are, were also known previously from broadband surface photometry (Strom *et al.* 1976; K. Strom and S. Strom 1978; Wirth 1981); in these studies, however, the nuclei were always excluded from analysis, and very "flat" changes, $\Delta[\text{Fe/H}]/\Delta\log r \approx -0.2$ (Peletier *et al.* 1990), were detected in the spheroid itself. What we found looked quite different: the

[*]E-mail: `olga@sai.msu.su`

$EW_{\mathrm{MgIb}}(r)$ profile had a sharp break at the boundary of the galactic nucleus determined by the seeing during the observations, and a jump in metallicity of more than $0.3-0.4$ dex was reached even at a radius of $R \approx 3''$. By analogy with the previously discovered kinematically decoupled nuclei (Jedrzejewski and Schechter 1988; Bender 1988; Afanasiev *et al.* 1989), we called this phenomenon a chemically decoupled nucleus; both these types of decoupling of the central region were present in several our objects, suggesting a special evolutionary status of the compact stellar nuclei of galaxies.

After 1992, we engaged in searching for and studying the chemically decoupled nuclei of galaxies in earnest; several dozen have now been found (Sil'chenko 2002a). The first version of MPFS was followed by two more modifications, and each succeeding modification was more efficient than the preceding one; the CCD detectors used on the spectrograph were also improved. We were among the first authors in the world to begin publishing two-dimensional maps of the Lick indices at the centers of galaxies (the Lick indices are the standardized equivalent widths of several absorption lines). By comparison with synthetic evolutionary models of stellar populations, for example, with the now classical models by Worthey (1994), we ascertained that, in addition to an enhanced metallicity, the chemically decoupled nuclei often have a younger mean age of the stellar population than do their surrounding bulges; i.e., they were clearly formed during a secondary starburst much later than the bulges. The first resolved chemically decoupled central structures similar in all signatures to circumnuclear compact stellar disks also appeared in our sample.

A serious limitation of our studies of chemically decoupled structures at the centers of galaxies performed so far has been the small field of view of our two-dimensional spectroscopy. In the latest version of MPFS, it is $16'' \times 16''$; if we encounter a decoupled circumnuclear disk with a radius of $5''-6''$, as in NGC 3384 (Sil'chenko *et al.* 2003) or NGC 3623 (Afanasiev and Sil'chenko 2004), we virtually run into the boundaries of the field of view and experience difficulties in decoupling the areas of the bulge with which we would like to compare the nuclei. Undoubtedly, two-dimensional spectroscopy with a larger field of view would help us to decoupling the chemically (and evolutionally) isolated part of a galaxy more reliably, to classify its morphology, and to determine whether this structure belongs to the classical large-scale galactic components. We got the opportunity to perform such an extensive analysis when the SAURON (Spectrographic Areal Unit for Research on Optical Nebulae) integral-field spectrograph at the William Herschel 4-m telescope was put into operation in the

Canary Islands in February 1999. The SAURON field of view is $41'' \times 33''$ or 44×38 spatial elements, with the size of a single pupil array element being $0.94'' \times 0.94''$. Although the spectrograph was declared to be a private instrument, its first data appeared in the publicly accessible archive of the UK Astronomy Data Centre a year after the first observations, and we were able to retrieve, analyze, and compare them with our data. The sample of 72 nearby galaxies compiled by the SAURON team for their first ambitious survey (de Zeeuw *et al.* 2002) overlapped with our sample by one third. We have now analyzed and published the SAURON data for five galaxies, including the above NGC 3384 and NGC 3623, in which the chemically decoupled nuclei are rather extended (several hundred parsecs) circumnuclear stellar disks. In this paper, we present the SAURON data for five more lenticular galaxies in which we claimed the existence of chemically decoupled nuclei previously based on MPFS data. Three of these, NGC 524, 1023, and 7332, appeared in our very first paper (Sil'chenko *et al.* 1992). Subsequently, they were once again studied with the second version of MPFS, and we again detected magnesium abundance peaks in their nuclei (Sil'chenko 1999, 2000). Thus, this work is a third approach to studying the central regions of these three galaxies by the method of integral-field spectroscopy. As regards NGC 4564 and NGC 7280, using MPFS, we found that their unresolved nuclei are not only chemically but also evolutionally decoupled: the stellar population in them is appreciably younger than that in their surrounding old stellar spheroids (Sil'chenko 1997; Afanasiev and Sil'chenko 2000). The global properties of the five galaxies recorded in the public databases considered in this paper are given in Table 1. Let us now consider how the large magnesium index maps provided by SAURON look for these galaxies.

SAURON: OBSERVATIONS AND DATA REDUCTION

The SAURON integral-field spectrograph was designed by an international team of researchers consisting mostly of representatives of France, the Netherlands, and Great Britain. A detailed description of the spectrograph and the team can be found in the paper by Bacon *et al.* (2001). The design of the spectrograph is based on the classical scheme of turning a lens array through a small angle relative to the direction of dispersion; this is called a TIGER mode in the literature. The second version of MPFS was also based on the same principle, which facilitated our work with SAURON data. In SAURON, a medium-band interference filter cuts out a spectral range of about $4800-5400$ Å; both the filter transmission curve and the reciprocal dispersion, within

Table 1. Global parameters of the five galaxies under study

NGC	524	4564	1023	7280	7332
Morphological type (NED[1])	SA(rs)0+	E6	SB(rs)0−	SAB(r)0+	S0 pec
R_{25}, arcmin (LEDA[2])	1.4	1.8	4.4	1.1	2.0
R_{25}, kpc	13.9	9.0	13.7	8.8	12.0
B_T^0 (RC3[3])	11.17	11.96	10.08	12.84	11.93
M_B (LEDA)	−21.63	−19.44	−20.23	−19.41	−19.16
$(B-V)_T^0$ (RC3)	1.00	0.90	0.93	0.85	0.87
$(U-B)_T^0$ (RC3)	0.58	0.45	0.50	0.37	0.38
V_r, km s^{-1} (NED)	2379	1142	637	1844	1172
Distance, Mpc	34.7	17.5	10.8	27.8	20.2
Line-of-sight inclination (LEDA)	8.4°	90°	90°	54°	90°
PA_phot (RC3)	−	47°	87°	78°	155°
σ_*, km s^{-1} (LEDA)	252	159	205	104	124
v_m(HI), km s^{-1} (LEDA)	−	−	190	131	136

[1] NASA/IPAC Extragalactic Database.
[2] Lyon−Meudon Extragalactic Database.
[3] Reference Catalogue of Bright Galaxies.

the range 1.11−1.21 Å/pixel, change slightly over the field of view. The sky is exposed simultaneously with an object on a single $4k \times 2k$ CCD detector and is taken at only 1.7′ from the center of the object under study. For large galaxies, this implies that the outer galactic regions are exposed instead of the sky. We took data for the five galaxies of interest, which were observed during three seasons from 1999 to 2000 (a list of exposure parameters is given in Table 2), from the publicly accessible ING (Isaac Newton Group) archive together with calibration data. Based on the comparison spectra of a neon lamp taken before and after each accumulation of the object, we extracted the spectra of spatial elements and linearized them using quadratic polynomials; the mean linearization accuracy was 0.07 Å. We corrected the spectral sensitivity variations over the field using exposures of a tungsten lamp and the different lens transmission using exposures of the twilight sky.

For the SAURON primary data reduction, we used a software package developed by Vlasyuk (1993) for MPFS data reduction and modified only slightly by the author to incorporate the peculiarities of the SAURON design. An original software package written in FORTRAN was used to compute the maps of absorption line indices; its basic element was a program written by A. Vazdekis; the program computes the Lick indices together with their statistical errors from the individual spectra of spatial

elements. Since the SAURON spectral resolution (4 Å) is much higher than the standard Lick resolution (∼8 Å), theoretically, the equivalent widths of the absorption lines, their objective characteristic, must be exactly equal to the computed indices. Nevertheless, we checked whether our Lick indices were the standard ones using the spectra of standard stars from the list by Worthey *et al.* (1994) that were observed during the same periods as the galaxies. The systematic deviations of our instrumental indices from the standard Lick values did not exceed 0.2 Å, and we applied these small systematic corrections to the measurements made for the galaxies. Based on the spectra of standard stars, we also studied what corrections should be applied to the measured indices to incorporate the line broadening in the spectra of the galaxies due to the stellar velocity dispersion. The spectra of giant stars were folded with a Gaussian of variable width, following which the indices were again measured from them and then compared with the indices measured from the "unspoiled" stellar spectrum. In this way, we established the dependence of the correction to the indices on σ_*; these dependences for each index were fitted with quadratic and cubic polynomials. For a typical stellar velocity dispersion of giant lenticular galaxies, ∼200 km s^{-1}, the corrections to the indices for the line broadening are 0.15 Å for Hβ, ∼0.3 Å for Mgb, and ∼0.6 Å

Table 2. SAURON spectroscopic observations of the five galaxies

Object	Date	$T_{\exp}$, min	$FWHM_*^{''}$
NGC 524	Sep. 4, 2000	3×30	1.4
NGC 1023, Position 1	Oct. 10, 1999	2×30	1.9
NGC 1023, Position 2	Oct. 10, 1999	2×30	1.9
NGC 1023, Position 3	Oct. 15, 1999	2×30	1.2
NGC 4564	Mar. 28/29, 2000	4×30	1.3
NGC 7280, Position 1	Sep. 3, 2000	3×30	1.4
NGC 7280, Position 2	Sep. 5, 2000	2×30	2.6
NGC 7332	Oct. 13, 1999	4×30	1.1

for Fe5270; for a velocity dispersion of ~ 100 km s^{-1}, which is observed in NGC 7280 and NGC 7332 (see Table 1), these corrections are negligible. The SAURON narrow spectral range is a great threat to the stability of the Fe5270 index system: even at moderate redshifts, $v_r \sim 1500-2000$ km s^{-1}, the Fe I+Ca I $\lambda 5270$ line shifts to the SAURON spectral sensitivity cutoff, and the Fe5270 index is found to be systematically underestimated. Therefore, we rely below on the Mgb index measurements when discussing how the chemically decoupled nuclei look in the SAURON data: the magnesium triplet with a mean wavelength of $\lambda 5175$ Å is in the middle of the SAURON spectral range and is measured most reliably.

To compute the stellar velocity field, we cross correlated the spectrum of each spatial element after the continuum subtraction and the transformation to the velocity scale with the spectra of K0−K2 giant stars observed during the same set as the galaxy. To determine the line-of-sight velocities of the gas, we measured the centroid position of the [OIII] $\lambda 5007$ emission line in the galaxies where it was intense enough.

THE NUCLEI DECOUPLED IN THE MAGNESIUM LINE

Based on SAURON data, we confirmed the existence of chemically decoupled nuclei in all five galaxies considered here. The high internal accuracy of the estimated absorption line indices, which reaches $0.02-0.03$ Å in the individual spatial elements of the central galactic regions and which is attributable to good statistics of the accumulated signal, makes this qualitative conclusion absolutely reliable.

In Fig. 1, we quantitatively compare the azimuthally averaged radial Mgb profiles derived from SAURON and MPFS data. Note particularly the agreement between the three Mgb profiles measured independently from SAURON data in NGC 1023 and the two Mgb profiles measured independently from MPFS data in NGC 7332: this allows us to immediately estimate the internal accuracy of the instruments by eye. The MPFS accuracy of the Mgb indices is approximately a factor of 3 lower than their SAURON accuracy. The break in the profiles at $R = 2''-4''$ is seen in the SAURON data even better than in the MPFS data: this is partly because of the higher accuracy of the data and partly because of the better atmospheric conditions and the higher spatial resolution of the observations. Good agreement between the quantitative Mgb estimates is also observed at the centers of the galaxies. However, in the outer (for MPFS) parts of the field, the MPFS magnesium indices are always found to be systematically lower than the SAURON ones. Since the only galaxy in which this discrepancy is absent, NGC 7280, is simultaneously the smallest galaxy in our sample, its angular radius is only 1.1′ (Table 1), the first thing that comes to mind is that the SAURON indices were overestimated due to the sky oversubtraction. Indeed, SAURON exposes the sky background at only 1.7′ from the galactic center, while the radius of NGC 1023 is, for example, 4.4′ (Table 1). It is clear that we subtracted not the pure sky background, but the sky background plus the galactic disk. This problem did not arise in the observations with the second version of MPFS, since the sky background was exposed separately far from the galaxy. If the magnesium line in the spectrum of the galactic disk is not as deep as that in the spectrum of the bulge because, for example, the stellar population of the disk is, on average, younger, then subtracting the "superfluous" continuum will lead to artificial line deepening, i.e., to the effect that can be seen in Fig. 1.
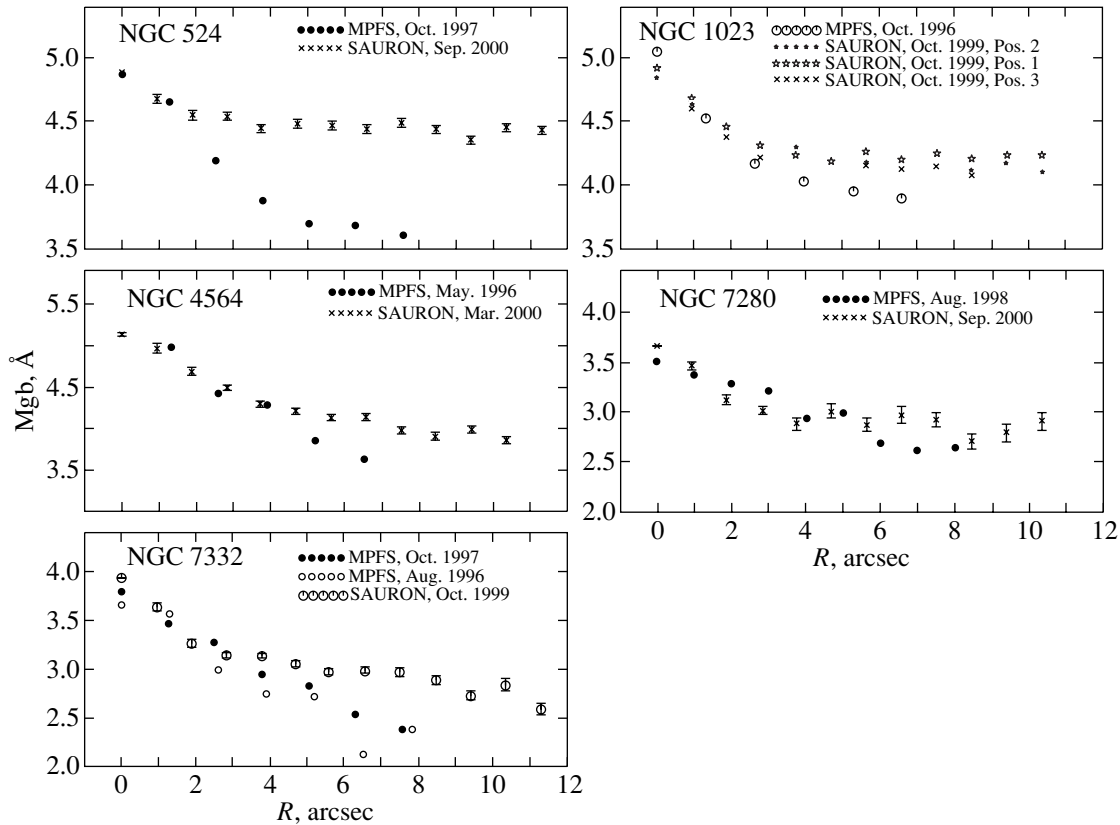
Fig. 1. Radial profiles of the azimuthally averaged Mgb absorption line index in the five galaxies under study from MPFS (which we published previously) and SAURON data.

However, this explanation in pure form is invalid: the radius of NGC 524 is only 1.4′, while the discrepancy between the MPFS and SAURON data is largest. Clearly, in addition to the sky oversubtraction in the SAURON data, the edge effects of the small field of the second MPFS version also play a role. Indeed, at a raster width of 8 elements and an element size of 1.3″, we have a full range of azimuths in the data of the second MPFS version when computing the azimuthally averaged profiles only up to a radius of 3″−4″; at larger radii, the rings open, the estimation accuracy decreases, and systematic errors appear. NGC 7280 is the only galaxy in our sample that was studied with the third version of MPFS with a 16″ × 16″ field of view. It has now become absolutely clear how important it was to confirm the existence of chemically decoupled nuclei in the galaxies using two-dimensional spectroscopy with a larger field of view than that in the first MPFS versions.

Based on Fig. 2, which shows two-dimensional distributions of the magnesium index, we can study the morphology of chemically and, hence, evolutionally decoupled substructures at the centers of galaxies. And here it emerges somewhat unexpectedly that the stellar structures decoupled in the magnesium line appear in most of the galaxies that we study as compact central knots virtually unresolved in observations. Why is this result unexpected? Because, for example, in NGC 4564 and NGC 7332, separate circumnuclear stellar disks with sizes that are quite resolvable in ground-based observations are known to exist from both photometric and kinematic studies. The radius of the central stellar disk is more than 10″ (see Pinkney *et al.* 2003, and references therein) in NGC 4564 and about 5″ (Seifert and Scorza 1996) in NGC 7332. One might expect that precisely the existence of circumnuclear stellar disks, the products of the secular evolution of disk galaxies, must cause the depth of the magnesium line to increase sharply in the integrated spectrum of the central galactic region. However, we see from Fig. 2 that the circumnuclear disks actually have magnesium indices higher than those of the bulge regions that dominate along the minor axis of the isophotes; compact knots in the nuclei, which are even more advanced in the sense of chemical evolution, are superimposed on these elongated regions. Clearly, although the secondary circumnuclear starburst often has a disk geometry, it is more effective at the distinguished point, at the geometric center of the galaxy.
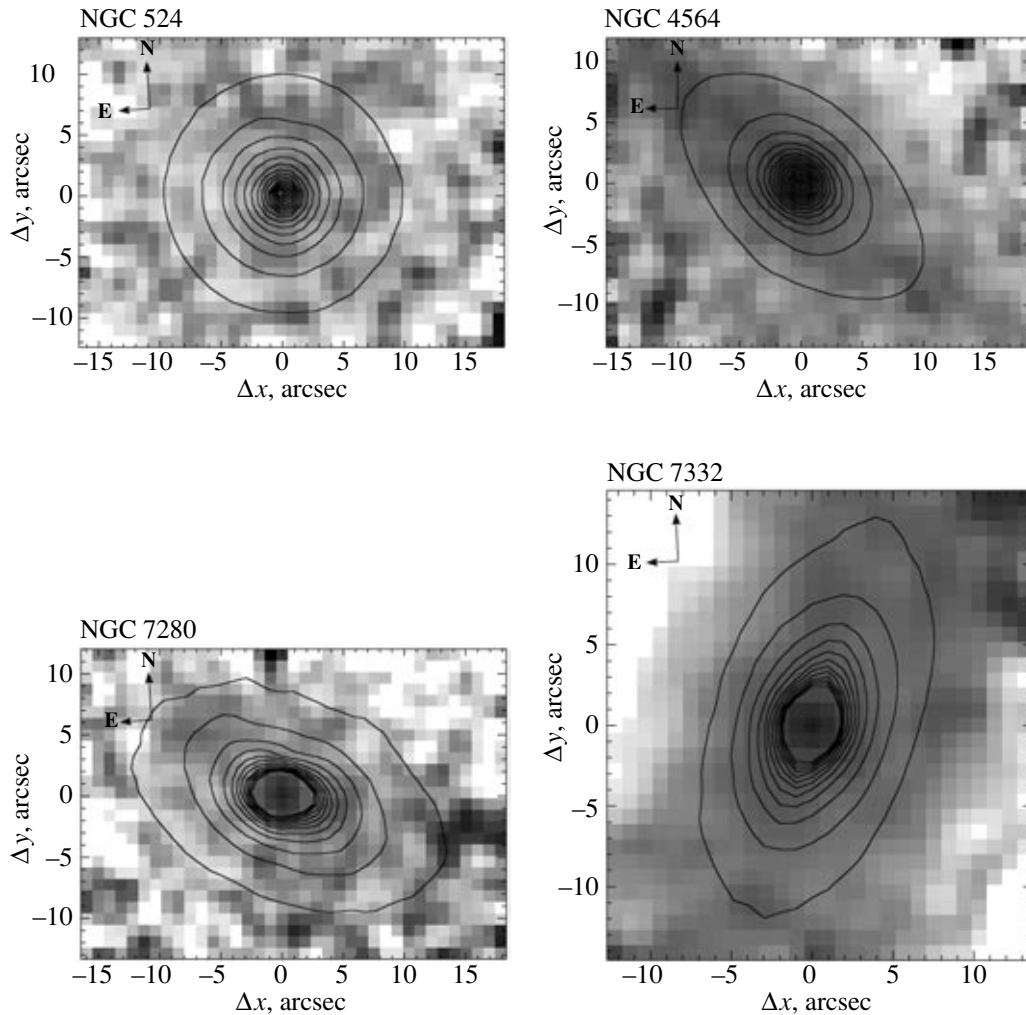
Fig. 2. Maps of the Mgb index in the central regions of four of the galaxies under study (the gray intensity scale); the superimposed isophotes indicate the continuum surface brightness distribution at $\lambda5000$ Å.

NGC 1023 constitutes a special, very curious case (Fig. 3). We see from Fig. 3a that the chemically decoupled nucleus is an elongated structure. In our previous paper on this galaxy (Sil'chenko 1999), we decided that we saw the circumnuclear disk edge-on, especially since the structure is elongated roughly along the line of nodes of the global galactic disk. However, we used no kinematic data in our analysis in that paper. Now, Fig. 3 also shows maps of the stellar velocity dispersion and line-of-sight velocities, and these data completely disprove the hypothesis of a circumnuclear disk decoupled in the magnesium line. Instead of the minimum of the stellar velocity dispersion at the center, evidence for the presence of a dynamically cold stellar disk observed, in particular, in NGC 3384 (Sil'chenko *et al.* 2003) or NGC 3623 (Afanasiev and Sil'chenko 2004), we see a maximum; the region of the maximum is not pointlike, as in galaxies where the gravity of a su-

permassive black hole dominates at the center, but is extended, elongated in a direction of $PA \approx 45°$. Such two-dimensional distributions of the stellar velocity dispersion can be observed at the centers of galaxies with old, dynamically evolved bars; in this case, the extended region of the maximum velocity dispersion is elongated along the bar (Vauterin and Dejonghe 1997). However, the same dynamical numerical models of bars also prescribe a turn of the lines of equal line-of-sight velocities of the ordered stellar motion along the bar, and we see from Fig. 3c that the isovelocities at the center of NGC 1023 turn in exactly the opposite direction, perpendicular to the elongation of the region of enhanced stellar velocity dispersion. To try to interpret this complex combination of orientations, let us compare the position angles of kinematic and photometric features. This comparison is shown in Fig. 4. Here, we used the photometric data obtained at different telescopes, with different
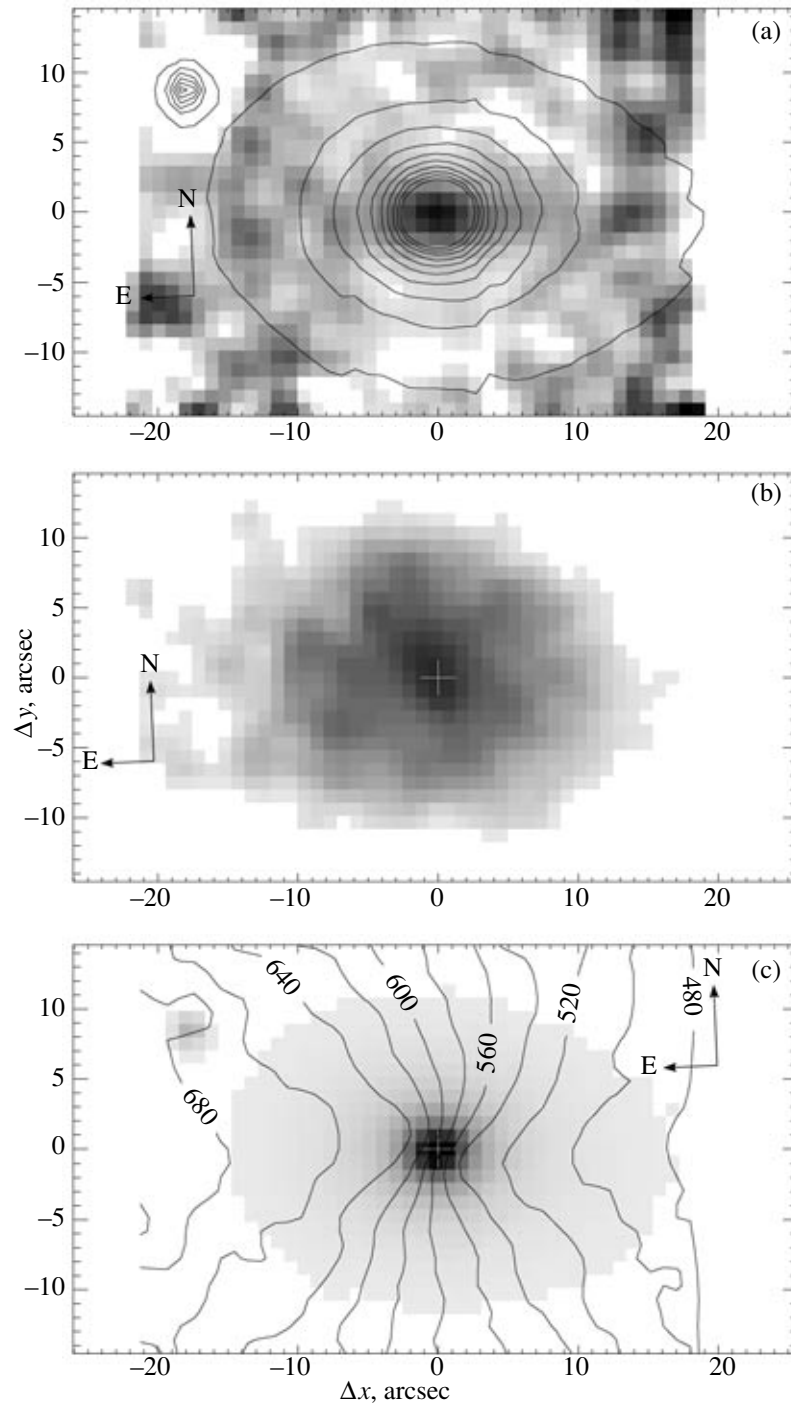
Fig. 3. SAURON data for NGC 1023: (a) the Mgb distribution, the superimposed isophotes indicate the continuum surface brightness distribution; (b) the distribution of stellar velocity dispersion; and (c) the lines of equal velocity (isovelocities) of the stellar line-of-sight velocity field superimposed on the continuum surface brightness map.

spatial resolutions, and in different spectral bands, from green (the $F555W$ filter on the WFPC2/HST camera) to near infrared (the K filter, $\lambda = 2\ \mu$m). All of these data are in excellent agreement at radii $R > 5''$, where the spatial resolution of the instrument does not distort the measurements. In addition to the posi-

tion angle of the isophotes, the dashed lines in Fig. 4 indicate the orientations of the lines of nodes of the bulge and the disk from Möllenhoff and Heidt (2001), while the solid line indicates the kinematic major axis (the direction of the maximum line-of-sight velocity gradient) of the stars, computed from the velocity
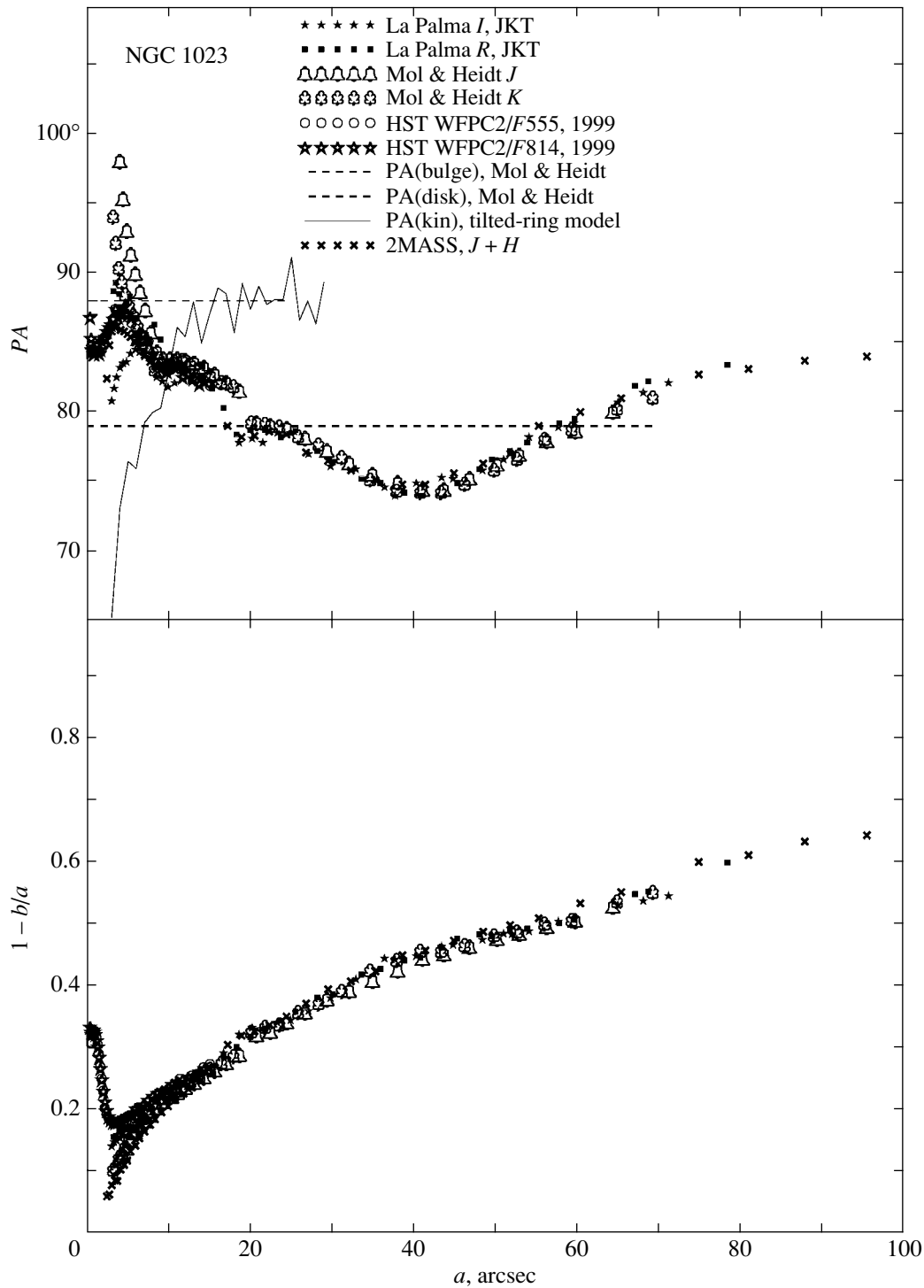
Fig. 4. Results of our isophotal analysis of the surface brightness distributions at various wavelengths in the galaxy NGC 1023, in the upper panel, in comparison with the orientation of the kinematic major axis of the stellar velocity field. We used optical photometric data from the Jacobus Kapteyn 1-m telescope at La Palma and the Hubble Space Telescope and near-infrared data published by Möllenhoff and Heidt (2001) and from the 2MASS survey.

field in Fig. 3 in terms of a tilted-ring model (Bege-man 1989) using the DETKA code written for IDL by A.V. Moiseev. The extrema in the $PA(R)$ dependence allow us to diagnose the existence of two elongated

photometric structures at the center of NGC 1023. The first, more compact structure with a radius of $\sim 5''$ is elongated in a direction of $PA \geq 88°$; it can be immediately identified with the structure decou-
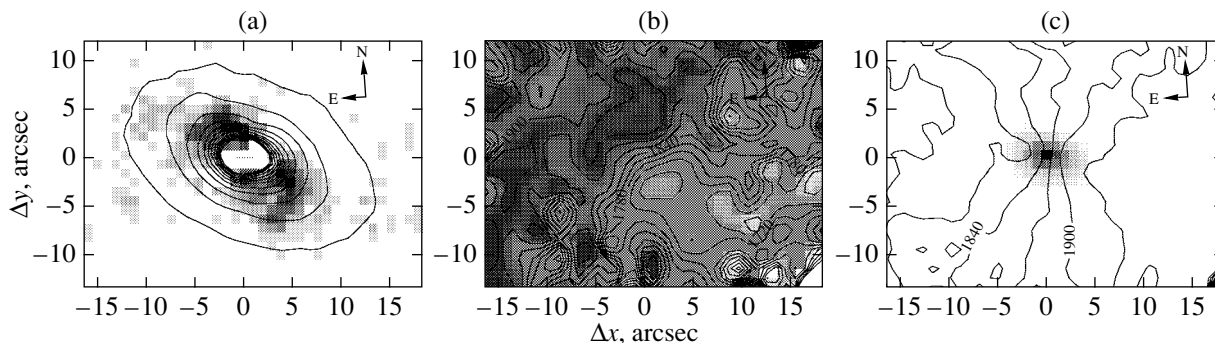
Fig. 5. Results of our SAURON data reduction for NGC 7280: (a) the gray intensity map of the [O III] $\lambda5007$ emission line with superimposed continuum surface brightness isophotes; (b) the ionized-gas velocity field (darker regions correspond to higher velocities; the superimposed isovelocities duplicate the gray-scale data); (c) the isovelocities of the stellar line-of-sight velocity field superimposed on the continuum surface brightness map.

pled in the magnesium line. The second elongated photometric structure in NGC 1023 has a radius of $\sim40''$ and a position angle of $PA \leq 74°$; clearly, this is just a global bar in the galactic disk, and the distribution of the stellar velocity dispersion is tied to it. Based on MPFS observations of a sample of 13 barred galaxies, Moiseev (2002) pointed out that the stellar velocity dispersion at the centers of even early-type galaxies traces the geometry of the global bar. And what is the nature of the central elongated structure? This is probably just the central part of the triaxial bulge of NGC 1023. That the bulge is triaxial follows at least from the fact that, according to Möllenhoff and Heidt (2001) and our Fig. 4, the major axis of its isophotes does not coincide with the line of nodes of the large galactic disk. In addition, in Fig. 4, the kinematic and photometric major axes at $R < 10''$ diverge in opposite directions relative to the line of nodes; this is a characteristic signature of rotation inside a triaxial potential (Monnet et al. 1992; Moiseev and Mustsevoĭ 2000). All scales are in agreement: according to Baggett et al. (1998), the bulge in NGC 1023 photometrically dominates over the disk at $R < 15''$, while according to Simien and Prugniel (1997), its dynamical influence is felt up to $R \sim 50''$; hence the agreement between the kinematic major axis and the photometric axis of the bulge in the range of radii $R \sim 15''-30''$.

THE INNER POLAR RINGS IN NGC 7280 AND NGC 7332

The circumnuclear gaseous polar rings in disk galaxies was a curious phenomenon that we encountered while looking for chemically decoupled nuclei by means of two-dimensional spectroscopy. Prior to our work, such rings were found only in galaxies of very early types; Bertola and Galletta (1978) introduced a special type of elliptical galaxies by distinguishing five objects with dust lanes along the minor axis. In elliptical galaxies without large-scale gaseous disks, the inner polar rings may well be assumed to result from the accretion of gas from another galaxy. We first discovered inner polar rings of ionized gas in several spiral galaxies (in NGC 2841 (Sil'chenko et al. 1997), NGC 7217 (Sil'chenko and Afanasiev 2000), NGC 6340 (Sil'chenko 2000), and NGC 4548 (Sil'chenko 2002b) where the outer gas is much greater in amount than the inner gas and rotates quite regularly in the symmetry plane of the galaxy together with the stars. This combination of nested noncoplanar gaseous disks is in much poorer agreement with the hypothesis of chance single-moment accretion. It has also emerged that the lenticular galaxies where we found inner polar rings, NGC 7280 (Afanasiev and Sil'chenko 2000) and eight more objects (Sil'chenko and Afanasiev 2004), are atypically rich in neutral hydrogen for this type of galaxies; the neutral gas is often concentrated near the plane of the galaxy, but outside its optical disk. When we compared the global structure of the galaxy with the phenomenon of a polar inner ring, we suspected that the concentration of the inner gas in polar orbits could be linked with the existence of a triaxial potential; this link, in particular, was previously suggested by some of the dynamical models by Friedli and Benz (1993).

Using the SAURON data, which have the advantage of a large field of view, we detected new features of the gas distribution and kinematics in galaxies with inner polar rings. Figures 5 and 6 show the results of our data reduction for NGC 7280 and NGC 7332: the line-of-sight velocity field of the gas (as measured in the [O III] $\lambda5007$ emission line) and stars as well as the emission surface brightness distribution against the background of the isophotes of the stellar distribution. In NGC 7280, we found an inner polar ring previously using MPFS data (Afanasiev and Sil'chenko 2000). In NGC 7332, we observed nothing
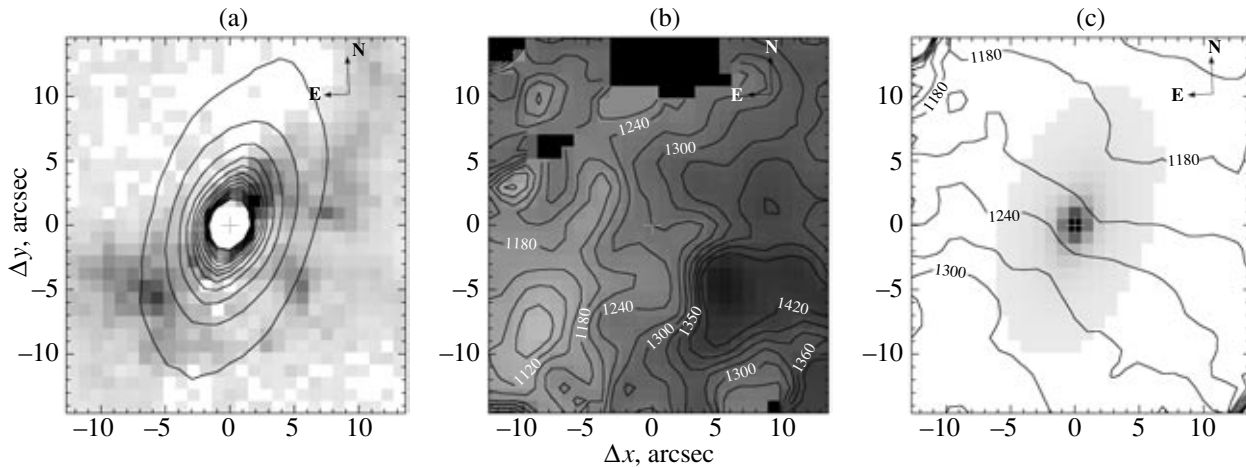
Fig. 6. Same as Fig. 5 for NGC 7332.

of this kind, although the galaxy was studied previously (Sil'chenko 1999). This is probably because the emission is absent in the nucleus itself, but appears only at about $5''$ from the center, which is an example of complex gas kinematics around a completely inactive nucleus. According to the SAURON data, the line-of-sight velocity field of the ionized gas in both galaxies is very complex, with a variable pattern of rotation at different distances from the center. A comparison of the gas and stellar velocity fields within $R = 5''-7''$ shows an almost polar rotation of the gas relative to the stars in both galaxies. Thus, for example, in NGC 7280, the position angles of the kinematic major axes of the stars and the gas in the ring $R = 2''-4''$ are $PA_{\mathrm{kin},*} = 261° \pm 0.5°$ and $PA_{\mathrm{kin},[\mathrm{O\,III}]} = 20° \pm 2°$, respectively; i.e., ΔPA is $\sim 120°$ (Fig. 5). In NGC 7332, the picture is not so distinct: the polar gas rotation cannot be traced in full azimuth; the red spot is best seen southwest of the nucleus, and the blue region is much less pronounced in the northeast with a velocity that, nevertheless, differs from the systemic velocity by ~ -100 km s^{-1} (Fig. 6). The polar gaseous ring of NGC 7332 with a hole inside is probably seen almost edge-on. However, the behavior of the gas at large ($R > 7''$) distances from the center is most curious: the maximum (along the azimuth) intensity of the emission at these radii is observed near the major axis of the continuum isophotes (in NGC 7280, this appears as a weak spiral; in NGC 7332, the gas distribution is more irregular), and the gas at $R > 10''$ within the SAURON field of view rotates in the opposite sense with respect to the stars in both galaxies. In NGC 7332, the extended counterrotating gaseous disk was described by Fisher *et al.* (1994); in NGC 7280, we point out this phenomenon for the first time.

DISCUSSION

The combination of an inner compact polar, or highly tilted, ring and an extended counterrotating gaseous disk coplanar to the stellar disk in a single galaxy has been first detected in our observations. However, it is most interesting that theoreticians predicted this combination long ago. Van Albada *et al.* (1982) considered the accretion of gas onto a rotating triaxial potential. At random mutual orientations of the initial momenta, the gas is eventually concentrated into a stably rotating disk in the plane perpendicular to the largest axis of the ellipsoid. However, since the potential figure rotates in space, the outer gaseous disk will be warped toward the plane orthogonal to the smallest axis of the ellipsoid in such a way that the gas rotates toward the stellar motion inside the ellipsoid. In contrast, another dynamical model, that of Friedli and Benz (1993), starts with the presence of a counterrotating gas in the global galactic disk. Internal instabilities in the stellar disk give rise to a bar; the gas in it gives up its momentum to the stars and sinks to the galactic center. If the gas initially counterrotated, its stable circumnuclear orbits would be highly inclined to the plane of the global disk. Falling to the center, the counterrotating gas escapes from the plane and is concentrated in a polar ring. Based on the currently available data alone, it is hard to say what appeared earlier, the chicken or the egg, i.e., the inner polar ring or the counterrotating gaseous disk. However, we do know that there are medium-sized bars, with a radius of $\sim 1-2$ kpc, in both NGC 7280 and NGC 7332. If this is the case, then the presence of an inner polar gaseous ring with a counterrotating outer gas is inevitable from the viewpoint of any of the models mentioned above.

Having analyzed the data for a factor of 3 to 5 larger field of view than we did previously with the

MPFS data, we confirmed the existence of chemically decoupled (in the magnesium line) nuclei in all five galaxies studied. However, the morphology of the chemically decoupled central regions turned out to be highly varied. In galaxies where the presence of separate circumnuclear stellar disks is known from photometric studies, these disks are also recognized in the distribution of the magnesium index; however, pointlike nuclei with a particularly strong magnesium line are superimposed on extended regions of enhanced metallicity. This inevitably suggests that the secondary starburst at the galactic center was nonuniform in space and, in these specific cases, was more effective in the nucleus than in the circumnuclear disk. In NGC 1023, a galaxy with a large bar, the central extended structure decoupled in the magnesium line turned out to be even not a disk, but a compact triaxial spheroid that is probably coaxial with the triaxial bulge. Whereas the current simulations often demonstrate possibilities for the formation of compact circumnuclear stellar disks during secondary central starbursts, the ways in which triaxial structures (minibars without disks?) are formed are so far completely unimaginable. We wish to emphasize the value of obtaining two-dimensional spectroscopic data for wide fields of view. Such data could allow us to accumulate larger statistical material on the morphology of evolutionarily decoupled structures at the centers of galaxies.

REFERENCES

1. V. L. Afanasiev and O. K. Sil'chenko, Astron. J. **119**, 126 (2000).
2. V. L. Afanasiev and O. K. Sil'chenko, Astron. Astrophys. **429**, 825 (2005).
3. V. L. Afanasiev, O. K. Sil'chenko, and A. V. Zasov, Astron. Astrophys. **213**, L9 (1989).
4. V. L. Afanasiev, V. V. Vlasyuk, S. N. Dodonov, and O. K. Sil'chenko, Preprint No. 54, SAO AN SSSR (Spec. Asrophys. Obs., Acad. Sci. USSR, Nizhniĭ Arkhyz, 1990).
5. R. Bacon, Y. Copin, G. Monnet, et al., Mon. Not. R. Astron. Soc. **326**, 23 (2001).
6. W. E. Baggett, S. M. Baggett, and K. S. J. Anderson, Astron. J. **116**, 1626 (1998).
7. K. Begeman, Astron. Astrophys. **223**, 47 (1989).
8. R. Bender, Astron. Astrophys. **202**, L5 (1988).
9. F. Bertola and G. Galletta, Astrophys. J. **226**, L115 (1978).
10. P. T. de Zeeuw, M. Bureau, E. Emsellem, et al., Mon. Not. R. Astron. Soc. **329**, 513 (2002).
11. D. Fisher, G. Illingworth, and M. Franx, Astron. J. **107**, 160 (1994).
12. D. Friedli and W. Benz, Astron. Astrophys. **268**, 65 (1993).
13. R. Jedrzejewski and P. L. Schechter, Astrophys. J. **330**, L87 (1988).
14. A. V. Moiseev, Pis'ma Astron. Zh. **28**, 840 (2002) [Astron. Lett. **28**, 755 (2002)].
15. A. V. Moiseev and V. V. Musstevoĭ, Pis'ma Astron. Zh. **26**, 657 (2000) [Astron. Lett. **26**, 565 (2000)].
16. C. Möllenhoff and J. Heidt, Astron. Astrophys. **368**, 16 (2001).
17. G. Monnet, R. Bacon, and E. Emsellem, Astron. Astrophys. **253**, 366 (1992).
18. R. F. Peletier, R. L. Davies, G. D. Illingworth, et al., Astron. J. **100**, 1091 (1990).
19. J. Pinkney, K. Gebhardt, R. Bender, et al., Astrophys. J. **596**, 903 (2003).
20. W. Seifert and C. Scorza, Astron. Astrophys. **310**, 75 (1996).
21. O. K. Sil'chenko, Astron. Zh. **74**, 643 (1997) [Astron. Rep. **41**, 567 (1997)].
22. O. K. Sil'chenko, Astron. J. **117**, 2725 (1999).
23. O. K. Sil'chenko, Astron. J. **120**, 741 (2000).
24. O. K. Sil'chenko, ASP Conf. Ser. **282**, 121 (2002a).
25. O. K. Sil'chenko, Pis'ma Astron. Zh. **28**, 243 (2002b) [Astron. Lett. **28**, 207 (2002b)].
26. O. K. Sil'chenko and V. L. Afanasiev, Astron. Astrophys. **364**, 479 (2000).

27. O. K. Sil'chenko and V. L. Afanasiev, Astron. J. **127**, 2641 (2004).

28. O. K. Sil'chenko, V. L. Afanasiev, and V. V. Vlasyuk, Astron. Zh. **69**, 1121 (1992) [Sov. Astron. **36**, 577 (1992)].

29. O. K. Sil'chenko, A. V. Moiseev, V. L. Afanasiev, *et al.*, Astrophys. J. **591**, 185 (2003).

30. O. K. Sil'chenko, V. V. Vlasyuk, and A. N. Burenkov, Astron. Astrophys. **326**, 941 (1997).

31. F. Simien and Ph. Prugniel, Astron. Astrophys., Suppl. Ser. **126**, 519 (1997).

32. K. M. Strom and S. E. Strom, Astron. J. **83**, 73 (1978).

33. S. E. Strom, K. M. Strom, J. W. Goad, *et al.*, Astrophys. J. **204**, 684 (1976).

34. T. S. Van Albada, C. G. Kotanyi, and M. Schwarzschild, Mon. Not. R. Astron. Soc. **198**, 303 (1982).

35. P. Vauterin and H. Dejonghe, Mon. Not. R. Astron. Soc. **286**, 812 (1997).

36. V. V. Vlasyuk, Izv. Spets. Astrofiz. Obs., Ross. Akad. Nauk **36**, 107 (1993).

37. A. Wirth, Astron. J. **86**, 981 (1981).

38. G. Worthey, Astrophys. J., Suppl. Ser. **95**, 107 (1994).

39. G. Worthey, S. M. Faber, J. J. Gonzalez, *et al.*, Astrophys. J., Suppl. Ser. **94**, 687 (1994).

Translated by V. Astakhov